

Elastic and Electronic Properties of Point Defects in Titanium Carbide

Dae-Bok Kang*

Department of Chemistry, Kyungsoong University, Busan 608-736, Korea

*E-mail: dbkang@ks.ac.kr

(Received September 11, 2013; Accepted October 29, 2013)

ABSTRACT. A theoretical study of the electronic structures of TiC_{1-x} and $\text{Ti}_{1-x}\text{W}_x\text{C}$ ($x = 0, 0.25$) is presented. The density of states and crystal orbital overlap population calculations were used to interpret variations of elastic properties induced by carbon vacancies and alloying substitutions. Our results show why the introduction of vacancies into TiC reduces bulk moduli, while W substitution at a Ti site increases the elastic modulus. The effect of the point defects on the bonding in TiC is investigated by means of extended Hückel tight-binding band calculations.

Key words: Electronic structure, Titanium carbide, Defects

INTRODUCTION

The transition metal (TM) carbides are attractive materials because of their novel mechanical, physical, and chemical properties. These compounds have extremely high melting points and hardness, including the machinability, as well as high thermal and electrical conductivity and chemical stability. The combination of such properties makes these materials potential candidates for a variety of high-temperature structural applications.¹⁻⁹ And TiC-based nanocomposites show a potential for superhard materials¹⁰ and have been found to provide enhanced toughness.¹¹

Many theoretical calculations have been made on these systems (see References 12–14 for comprehensive experimental and theoretical reviews). The bonding features that have been clarified in these studies are useful in interpreting their physical properties. The common viewpoint is that covalent bonds can be formed between both metal–carbon and metal–metal pairs of atoms. At the same time, a transfer of electrons from metal to carbon takes place, implying a certain degree of ionic bonding. We stress the importance of the covalency of metal–carbon bonds in explaining the stability and observed mechanical properties of these compounds.¹⁵ Specifically, the elastic behavior of the TM carbides is understood to arise in large part from strong covalent bonding between transition metal *d* and carbon *p* orbitals.

Cubic TiC, which is the subject of study here, is an important thin film material commonly used as protective coating layers and it is also regarded as a prototype refractory TM carbide. The cubic rocksalt-type TiC normally exists in nonstoichiometric phases with a substantial amount of

vacancies in the carbon sublattice.^{1,16} The vacancies have very high diffusion barriers which are important for the stability of carbides.¹⁷ This implies that once nonstoichiometric films are formed, the lattice stays intact because vacancies do not hop to other sites.

Electronic changes induced by vacancies in TiC have been studied with X-ray photoemission spectra.¹⁶ Theoretical calculations on nonstoichiometric TiC have been done on cubic $\text{TiC}_{0.75}$ samples by Redinger et al.¹⁸ using a self-consistent augmented plane wave (APW) method and a model structure with ordered vacancies not allowing for local relaxations around the vacancies. More recently the relaxation of the atoms around the vacancies in nonstoichiometric TiC_{1-x} has been investigated by Tan et al.¹⁹ using a tight-binding model. Hugosson et al.²⁰ employed a combination of a pseudo-potential plane wave approach and the full-potential linear muffin-tin method to study the energetics and structural properties for various configurations of nonstoichiometric TiC_x . They have demonstrated that vacancies induce the creation of new bonding states between the metal atoms surrounding the vacancy below the Fermi level.

Alloying additions in TM carbides have not been much studied experimentally. Theoretical studies on them are also relatively rare. The electronic properties of $\text{TiC}_x\text{N}_{1-x}$ alloys were calculated by Zhukov et al.,²¹ and the structural stability and elastic stiffness of these alloys were studied by Jhi et al.,²² using the ab initio pseudopotential approach. Recently, Liu et al. investigated the mechanical and electronic behavior of binary TiC and its ternary alloys.²³ Tungsten is the element added to improve the ductility of TiC. Its importance stems from the search for

new materials with superior tribotechnical properties, which would simultaneously combine substantial hardness with a certain plasticity. The elastic properties of the ternary carbides $\text{Ti}_{1-x}\text{W}_x\text{C}$ differ significantly from the host TiC. Alloying substitutions in TiC affect mechanical properties, such as elastic moduli and hardness. The ternary carbide system is thus of considerable theoretical and practical interest. To learn more about the bonding nature of these binary and ternary carbides, a detailed theoretical investigation into the mechanical and electronic behavior must be conducted.

As all these properties are primarily linked to the electronic band structure, we study the variations of the valence band structure of TiC in the rocksalt structure by W substitution at Ti sites and C vacancies and their effects on the elastic properties. These point defects in TiC will introduce significant changes in the covalent bonding involving the C 2p and Ti 3d orbitals. The purpose of our study is to

understand, in terms of electronic properties, the mechanical properties of TM carbides. This understanding is crucial to the design of hard materials based on these compounds.

In the present paper, we focus on the electronic structures of the nonstoichiometric $\text{TiC}_{0.75}$ phase and the ternary compound $\text{Ti}_{0.75}\text{W}_{0.25}\text{C}$. The goal of this work is to gain insight into the chemical bonding of these systems. Chemical bonding is discussed in terms of the total, projected density of states (DOS), and crystal orbital overlap population (COOP). The COOP curves are indicative of the nature and strength of the bonding between a given pair of atoms, with positive and negative regions indicating bonding and antibonding states, respectively. We study quantitatively the chemical bonding of metal–carbon and metal–metal by use of the integrated overlap populations. All calculations in this work have been performed using the extended Hückel tight-binding (EHTB) method;^{24,25} atomic parameters are given in Table 1.

Table 1. Parameters for EH calculations

Atom	Orbital	H_{ii} , eV	ζ_1^b	ζ_2^b	c_1^a	c_2^a
W	5d	−10.37	4.982	2.068	0.6940	0.5631
	6s	−8.26	2.341			
	6p	−5.17	2.309			
Ti	3d	−10.81	4.55	1.40	0.4206	0.7839
	4s	−8.97	1.5			
	4p	−5.44	1.5			
C	2s	−21.4	1.625			
	2p	−11.4	1.625			

^aCoefficients used in double- ζ expansion.

^bSlater-type orbital exponents.

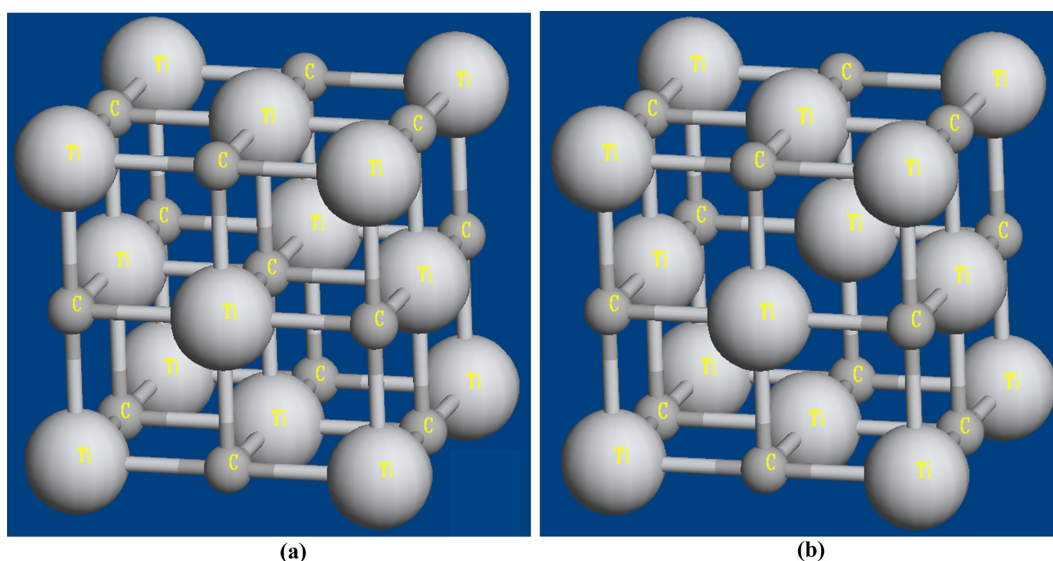


Figure 1. Unit cells for (a) stoichiometric TiC and (b) ordered vacant model structure $\text{TiC}_{0.75}$ (Ti: large spheres, C: dark small spheres).

RESULTS AND DISCUSSION

Structural and Elastic Properties

TiC crystallizes in the NaCl-like face-centered cubic structure with $Fm\bar{3}m$ (O_h) space group (No. 225). Ti atoms occupy $4a$ -sites at origin, C atoms occupy $4b$ -sites at $(1/2, 1/2, 1/2)$, and thus the conventional unit cell contains four TiC formula units shown in Fig. 1. A model structure of 8 atom supercell, periodically repeated in three dimensions, is used for the present calculations. Nonstoichiometric $\text{TiC}_{0.75}$ and $\text{Ti}_{0.75}\text{W}_{0.25}\text{C}$ are simulated by substituting a vacancy on one C atom and a W on one Ti atom in the unit cell, respectively. The W-doping is performed via the gradual substitutions of Ti with W. We thus have Ti_3WC_4 for $\text{Ti}_{0.75}\text{W}_{0.25}\text{C}$ and $\text{Ti}_2\text{W}_2\text{C}_4$ for $\text{Ti}_{0.5}\text{W}_{0.5}\text{C}$. The vacancy creation divides the metal atoms into two groups (i.e., Ti6 and Ti4) according to the coordination number. The vacancy is octahedrally surrounded by six Ti4 atoms which have only four nearest C neighbors. The Ti6 atoms are surrounded by six C neighbors as in stoichiometric TiC. To discern the salient bonding characteristics associated with these point defects, the lattice parameter in our calculations is assumed to be fixed at the value ($a_0 = 4.331\text{\AA}$) equal to the theoretically determined lattice constant of the binary carbide TiC.²³

The lattice parameters and bulk moduli are summarized in Table 2. The vacancy creation in TiC decreases bulk modulus,²⁶ while the W-doping in TiC increases bulk modulus.²³ We discuss below in detail the effect of C vacancies and W/Ti substitutions on the electronic and bonding properties of TiC.

Electronic and Bonding Properties

Carbon vacancies

We present the valence band DOS spectra of TiC_{1-x} carbides for the different C concentrations $x = 0$ and $x = 0.25$. The vacancy effects on the electronic structure of TiC are more closely examined in this section. The ordered vacancy defects are modeled by removing a carbon atom from the 8 atom supercell. In the case of TiC with no defects present, each metal atom has an octahedral environment of six sites in the carbon sublattice. For comparison Fig.

Table 2. Calculated lattice constants (a_0) and bulk moduli (B) for TiC, $\text{TiC}_{0.75}$, and $\text{Ti}_{0.75}\text{W}_{0.25}\text{C}$ ²³

	TiC	$\text{TiC}_{0.75}$ ^a	$\text{Ti}_{0.75}\text{W}_{0.25}\text{C}$
a_0 (Å)	4.331 (4.275) ^a	4.252	4.330
B (GPa)	250 (277) ^a	247	287 (253) ^b

^aReference 26.

^bReference 28.

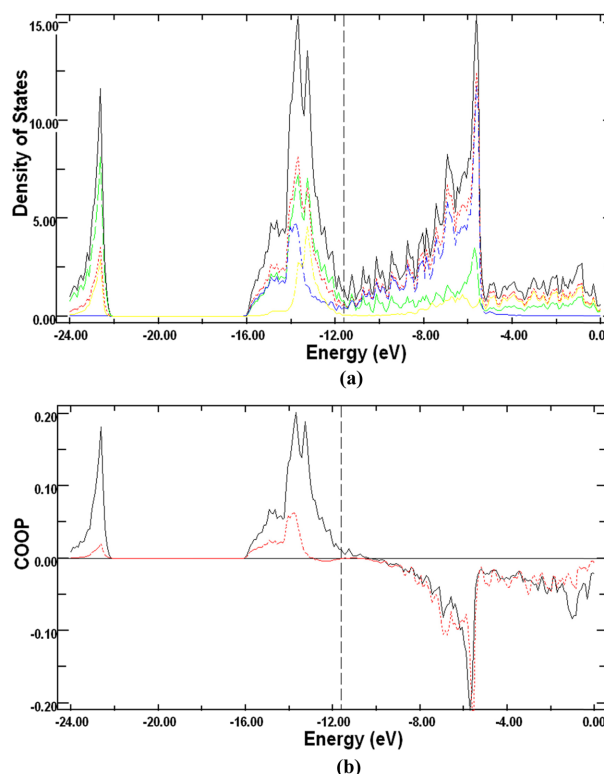


Figure 2. (a) Total DOS (black line) and the contributions of Ti (red line), C (green line), t_{2g} (blue line), and e_g (yellow line) orbitals to it in TiC. (b) Crystal orbital overlap populations for Ti-C (black line) and Ti-Ti (red line) bonds in TiC. The Fermi level is indicated by a vertical dashed line.

2(a) show the calculated DOS of stoichiometric TiC which is decomposed into three main regions. The deeply bound lowest valence band (LVB) is mainly built of the C 2s states with a small contribution of the Ti 3d states. At higher energies, one observes three overlapping bands (-14.7 eV, -13.7 eV, and -13.3 eV) separated from the C 2s band by an energy gap. These filled upper valence bands (UVB) originate from C 2p states and contains also appreciable Ti 3d states, indicating a strong interaction between C 2p and Ti 3d orbitals. Finally, at higher energies, above the Fermi level (E_F), appears the conduction band (CB) derived from the Ti 3d states which are mostly mixed with C 2p states. This d band consists of two components t_{2g} and e_g . The t_{2g} of the band is situated at lower energies. The Fermi level falls at the bottom of wide minimum in the DOS and separates approximately the p(C)-d(Ti) bonding from the d-d nonbonding states, exhibiting strong Ti-C covalent bonding behavior. As for the great majority of the TM carbides, there is no band gap and the DOS has a finite value at E_F . This confirms the metallic properties of TiC. As shown in Fig. 2(b), the states below E_F are derived from strongly

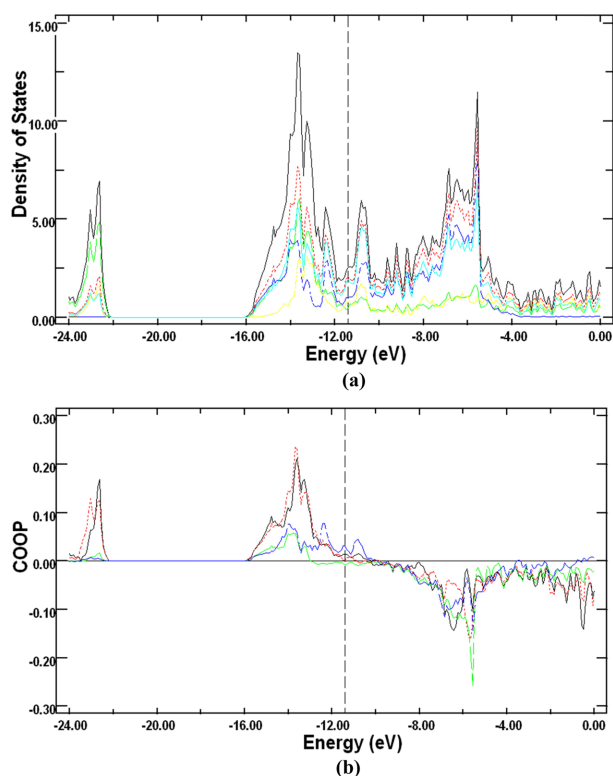


Figure 3. (a) Total DOS (black line) and the contributions of Ti (red line), C (green line), t_{2g} (blue line), e_g (yellow line), and Ti4 (light blue) orbitals to it in $\text{TiC}_{0.75}$. (b) Crystal orbital overlap populations for Ti6–C (black line), Ti4–C (red line), Ti6–Ti4 (green line), and Ti4–Ti4 (blue line) bonds in $\text{TiC}_{0.75}$. The Fermi level is indicated by a vertical dashed line.

mixed bonding combinations of C 2p and Ti 3d orbitals, with some contribution from Ti–Ti t_{2g} σ bonding states. Both the corresponding antibonding components lie in the unoccupied region (ca. -5.6 eV). The t_{2g} orbitals interact with neighboring Ti t_{2g} orbitals of the same symmetry to create d–d σ -type bonds. Since the e_g orbitals are strongly antibonding in their interaction with appropriate orbitals of the neighboring C atoms, the e_g band is situated high above -5.6 eV. Thus, the DOS and COOP results of the stoichiometric TiC phase provide evidence for both metallic and covalent Ti–C bonding.

When carbon vacancies are introduced, the change in the DOS is seen in Fig. 3(a) for $\text{TiC}_{0.75}$. The most striking feature is the appearance of two new well resolved peaks in the vicinity of the Fermi level. These distinct peaks appear about 1.0 eV below the Fermi level and 0.6 eV above E_F . The two peaks are worth noting because these structures can be interpreted as being associated with the so-called vacancy states which dominate near the Fermi level. Fig. 3(a) also displays the Ti4 and Ti6 contributions

to the total DOS. We see that the vacancy states arise mainly from t_{2g} orbitals of the four-coordinated Ti4 atoms. The antibonding Ti d states containing contribution from carbon p orbitals are lowered by the removal of the carbon atom. The intensity of the sharp Ti t_{2g} peak located at -5.6 eV in TiC is reduced by the introduction of carbon vacancies. Therefore, the vacancy-induced peaks are associated with octahedral Ti–Ti covalent bonding between the immediate Ti neighbors (i.e., Ti4) of the vacancy site, formed primarily by the Ti 3d states from broken Ti–C bonds. In particular, the presence of a rather strong vacancy peak right below E_F has a discernible effect on the mechanical and electronic properties of the nonstoichiometric phase. Searching for electronic reasons behind the remarkable properties of this class of materials, one must focus on the filled bonding states. In $\text{TiC}_{0.75}$, the electrons occupy the localized vacancy states near the Fermi level as shown in Fig. 3(b). This occupancy confirms that the nonstoichiometric phase is favored energetically. In addition, this results in the increase in the bond strength between the neighboring Ti4 atoms surrounding the vacancy and is believed to be an important factor in determining the bulk modulus. The strengthening of the metallic bonds between the Ti atoms nearest to the vacancy site causes a change in the cohesion of the studied $\text{TiC}_{0.75}$ compound and affects the bulk modulus. Consequently, the introduction of vacancies into stoichiometric TiC makes this compound more compressible, which reduces bulk modulus and leads to a less hard compound. The bulk moduli, which exhibit elastic properties, are given in Table 2. Compared with TiC, $\text{TiC}_{0.75}$ has a lower value in bulk modulus.²⁶

The overlap population (OP) is used to characterize the strength of a covalent bond. The bond strength can be determined by the total overlap population obtained by summing up the area under the COOP curve up to the Fermi level. The overlap populations calculated for a pair of atoms in unit cells are given in Table 3. Although the same bonds can be compared for the two systems, we cannot directly compare the strength of the Ti–C and Ti–Ti bonds, because the overlap population changes with the different bond length and geometry arrangement. Since the C–C distance is more than twice larger than the sum of the covalent radii of carbon (1.54 Å), the interaction between two carbon atoms is negligible. The carbon atoms are thus bound in the structure only via interaction with nearest-neighbor metal atoms. The C 2p–Ti 3d bonding interaction is so strong that the overlap population between them gives a large value. In TiC, the OP of the Ti–C bond is 0.43, while that of the Ti–Ti bond is 0.08. The Ti–Ti dis-

Table 3. Overlap populations (OP) for a pair of atoms in TiC, TiC_{0.75}, Ti_{0.75}W_{0.25}C, and Ti_{0.5}W_{0.5}C

Compound	Bond	Bond Length (Å)	OP
TiC	Ti–C	2.17 (2.10) ^a	0.43
	Ti–Ti	3.06 (2.65)	0.08
TiC _{0.75}	Ti6–C	2.17	0.42
	Ti4–C	2.17	0.44
	Ti4–Ti6	3.06	0.08
	Ti4–Ti4	3.06	0.16
Ti _{0.75} W _{0.25} C	Ti–C	2.17	0.46
	W–C	2.17 (2.08)	0.35
	Ti–Ti	3.06	0.08
	W–Ti	3.06 (2.63)	0.06
Ti _{0.5} W _{0.5} C	Ti–C	2.17	0.49
	W–C	2.17	0.37
	Ti–Ti	3.06	0.09
	W–Ti	3.06	0.07
	W–W	3.06 (2.61)	0.05

^aThe sum of single-bond radii for a given pair of atoms is presented in parentheses.²⁷

tance is much longer than the nearest-neighbor distance in pure metals. This indicates weak d–d interactions between Ti atoms in contrast to the strong p(C)–d(Ti) interaction. For TiC_{0.75}, two types of Ti atoms (i.e., Ti4 and Ti6) enter the Ti–C bonding interactions. The Ti6–C and Ti4–C bonds have slightly different overlap populations of 0.42 and 0.44, respectively. Note that the Ti4–C bond strength is slightly larger than the Ti6–C one. This is caused by an increasing amount of the Ti4 d orbitals included in these bonds. The reason for this increasing is due to the formation of the Ti4–Ti4 bonds strengthened via the vacancy. The overlap population for Ti4–Ti6 differs very little from that for the Ti6–Ti6. From Table 3, it should be pointed out that the Ti4–Ti4 bond has a considerably higher OP value (0.16) than that of the Ti4–Ti6 bond (0.08). This means that the Ti4 atoms with lowered coordination number create metal–metal bonds which are strengthened. The occupied vacancy states situated on the Ti4 atoms are directed towards the neighboring Ti atoms nearest to the carbon vacancy site and their relaxations towards the vacancy site can be expected. The strengthening of the Ti4–Ti4 bonds may thus result in the lower bulk modulus of TiC_{0.75} than that of TiC.

Tungsten substitutions

We now turn our attention to the mechanism of alloying effects on elastic properties of Ti_{1-x}W_xC (x = 0.25, 0.5). In the W-doped TM carbide, the W replaces Ti atoms. One W/Ti substitution in the supercell with 4 Ti atoms results

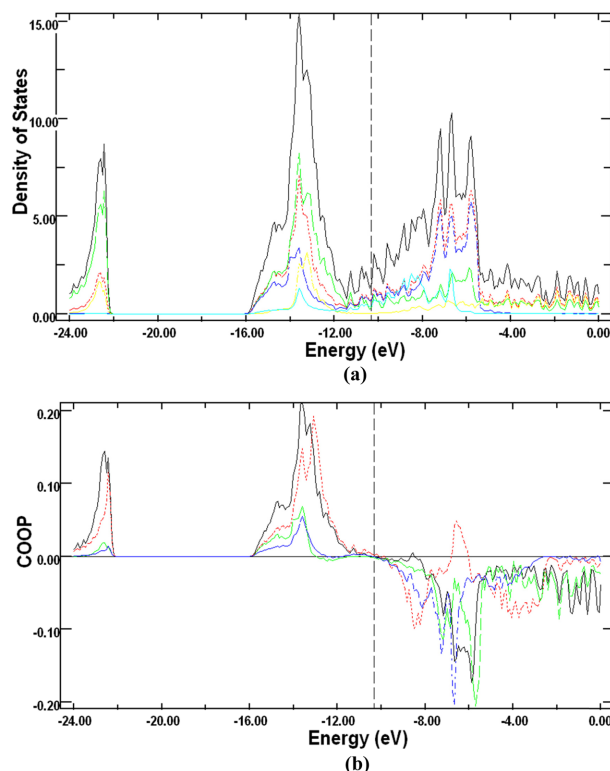


Figure 4. (a) Total DOS (black line) and the contributions of Ti (red line), C (green line), Ti t_{2g} (blue line), Ti e_g (yellow line), and W t_{2g} (light blue) orbitals to it in Ti_{0.75}W_{0.25}C. (b) Crystal orbital overlap populations for Ti–C (black line), W–C (red line), Ti–Ti (green line), and W–Ti (blue line) bonds in Ti_{0.75}W_{0.25}C. The Fermi level is indicated by a vertical dashed line.

in a composition Ti_{0.75}W_{0.25}C. It is worthy of notice that the chemical bond between Ti and C atoms is strengthened as the concentration of alloying element W is increased from x = 0 to x = 0.5. In order to further explore the bonding behavior between metal–metal and metal–carbon atoms, the projected DOS for Ti, C, and W atoms and the COOP between them are calculated. Fig. 4(a) clearly shows the dominating covalent bonding between the Ti 3d and the C 2p orbitals in Ti_{0.75}W_{0.25}C. The W/Ti substitution does not change the electronic structure significantly. The shape and location of UVB and CB peaks are virtually unchanged in transition from TiC to Ti_{0.75}W_{0.25}C. The UVB and CB are mainly derived from the C 2p and Ti 3d states resulting from the strong mixing between the C 2p and Ti 3d orbitals, respectively. An important aspect of the W substitution is that a full occupation of the unfilled states near the bottom of CB takes place in this case. In case of TiC, the UVB is not fully filled with eight valence electrons. The substitution of Ti by W increases the number of valence electrons and the additional valence electrons cause the

Fermi level to shift towards higher energies. This high-energy shift of E_F populates electrons in all the bonding states just below the Fermi level as shown in Fig. 4(b). A larger occupation of the Ti 3d–C 2p bonding states accounts for the higher Ti–C bond strength of the ternary carbide system. Note that the OP value of the Ti–C bond in $Ti_{0.75}W_{0.25}C$ is larger than that in TiC (see Table 3). There is an additional bonding interaction contributed by W, filling the W 5d–C 2p bonding states in the UVB region. Their antibonding states are empty. The bonding interaction between C 2p and Ti 3d states is stronger than that between C 2p and W 5d states. This can be attributed to the shifts to lower energies of the DOS peaks of the C 2p states with Ti d contribution relative to the W d. As shown in Fig. 4(b), the UVB consists of p–d bonding states and the CB just above E_F comprises d–d nonbonding and p–d antibonding states. The p–d bonding and antibonding peaks for Ti–C are more apart in energy compared to those for W–C. The larger p–d bonding–antibonding splitting for Ti–C reflects the higher bond strength of Ti–C relative to W–C. On the other hand, some electrons are also populated in the Ti and W d states that build bonds between the Ti–Ti and Ti–W atoms. The net result leads to a rising of the bulk modulus in $Ti_{0.75}W_{0.25}C$ in comparison with TiC. The variation of bulk modulus follows the strength of the covalent bonding between titanium and carbon in the studied carbides.

In the $Ti_{0.5}W_{0.5}C$ system, the value of bulk modulus is expected to increase due to the increase in the strength of the Ti–C bonds, demonstrated by the increased OP values. The calculated OP values of the W-doped ternary carbides are listed in Table 3. These results indicate that alloying substitutions of titanium with tungsten enhance the bond strength between titanium and carbon in the ternary carbide. Depending how strong the Ti–C covalent bonds are, the mechanical properties of the materials can be different. The stronger the covalent bonding the higher is the resistance to elastic deformation reflected in the bulk modulus. Thus, the elastic properties of TM carbides can be explained by the strong covalent bonding of metal d and carbon p orbitals. As deduced from our OP values, the Ti–C covalency of $Ti_{0.5}W_{0.5}C$ is higher than that of $Ti_{0.75}W_{0.25}C$. Therefore, it is expected that the hardness should be higher for $Ti_{0.5}W_{0.5}C$ than for $Ti_{0.75}W_{0.25}C$.

CONCLUDING REMARKS

To conclude, we have studied the elastic and electronic properties of TiC_{1-x} and $Ti_{1-x}W_xC$ ($x = 0, 0.25$) compounds by means of EHTB band calculations. Two point defects

were considered: C vacancies and W substitutions at Ti sites in TiC. The introduction of carbon vacancies in TiC induces new DOS peaks near the Fermi level which are due to the Ti d–Ti d bonding states between neighboring titanium atoms around vacancies. Filling of the vacancy-induced states strengthens the Ti–Ti bonds between the nearest Ti neighbors of the vacancy site and causes only a slight decrease of the bulk modulus. As the concentration of alloying W atoms is increased in the studied ternary system, we observe the strengthening of the covalent Ti–C bond due to an increase in the number of valence electrons of metal atoms. The increase in the Ti–C bond strength correlates with the enhancement of the bulk modulus in the ternary carbide system.

Acknowledgments. This work was supported by the Kyungshung University Research Grant in 2013.

REFERENCES

- (a) Toth, L. E. *Transition Metal Carbides and Nitrides*; Academic Press: New York, 1971. (b) Dunand, A.; Flack, H. D.; Yvon, K. *Phys. Rev. B* **1985**, *31*, 2299. (c) Pollini, I.; Mosser, A.; Parlebas, J. C. *Phys. Rep.* **2001**, *355*, 1.
- Pierson, H. O. *Handbook of Refractory Carbides and Nitrides*; Noyes Publishing: New Jersey, 1996.
- Gagnon, G. *J. Appl. Phys.* **1996**, *79*, 7612.
- Nowak, R.; Li, C. L. *Thin Solid Films* **1997**, *305*, 297.
- Zhukov, V. P.; Gubanov, V. A.; Jepsen, O.; Christensen, N. E.; Anderson, O. K. *J. Phys. Chem. Solids* **1988**, *49*, 841.
- Opeka, M. M.; Talmy, I. G.; Zaykosk, J. A. *J. Mater. Sci.* **2004**, *39*, 5887.
- Levine, S. R.; Opila, E. J.; Halbig, M. C.; Kiser, J. D.; Singh, M.; Salem, J. A. *J. Eur. Ceram. Soc.* **2002**, *22*, 2757.
- Isaev, E. I.; Ahuja, R.; Simak, S. I.; Lichtenstein, A. I.; Vekilov, Y. K.; Johansson, B.; Abrikosov, I. A. *Phys. Rev. B* **2005**, *72*, 064515.
- Isaev, E. I.; Simak, S. I.; Abrikosov, I. A.; Ahuja, R.; Vekilov, Y. K.; Katsnelson, M. I.; Lichtenstein, A. I.; Johansson, B. *J. Appl. Phys.* **2007**, *101*, 123519.
- Musil, J. *Surf. Coat. Technol.* **2000**, *125*, 322.
- Wen, G.; Li, S. B.; Zhang, B. S.; Guo, Z. X. *Acta Mater.* **2001**, *49*, 1463.
- Schwarz, K. *CRC Crit. Rev. Solid State Mater. Sci.* **1987**, *13*, 211.
- Johansson, L. I. *Surf. Sci. Rep.* **1995**, *21*, 177.
- Williams, W. S. *Mater. Sci. Eng. A* **1988**, *105/106*, 1.
- Kang, D.-B. *Bull. Korean Chem. Soc.* **2013**, *34*, 609; **2013**, *34*, 2171.
- Guemmaz, M.; Mosser, A.; Parlebas, J. C. *J. Electron. Spectrosc. Relat. Phenom.* **2000**, *107*, 91.
- Tsetseris, L.; Kalfagiannis, N.; Logothetidis, S.; Pantelides, S. T. *Phys. Rev. Lett.* **2007**, *99*, 125503.

18. Redinger, J.; Eibler, R.; Herzig, P.; Neckel, A.; Podlucky, R.; Wimmer, E. *J. Phys. Chem. Solids* **1985**, *46*, 383.
 19. Tan, K. E.; Bratkovsky, A. M.; Harris, R. M.; Horsfield, A. P.; Nguyen-Mahn, D.; Pettifor, D. G.; Sutton, A. P. *Model. Simul. Mater. Sci. Eng.* **1997**, *5*, 187.
 20. Hugosson, H. W.; Korzhavyi, P.; Jansson, U.; Johansson, B.; Eriksson, O. *Phys. Rev. B* **2001**, *63*, 165116.
 21. Zhukov, V. P.; Gubanov, V. A.; Jepsen, O.; Christensen, N. E.; Andersen, O. K. *Phil. Mag. B* **1988**, *58*, 139.
 22. Jhi, S.-H.; Ihm, J.; Louie, S. G.; Cohen, M. L. *Nature* **1999**, *399*, 132.
 23. Wang, B.; Liu, Y.; Liu, Y.; Ye, J.-W. *Physica B* **2012**, *407*, 2542.
 24. Whangbo, M.-H.; Hoffmann, R. *J. Am. Chem. Soc.* **1978**, *100*, 6093.
 25. Whangbo, M.-H.; Hoffmann, R.; Woodward, R. B. *Proc. R. Soc. A* **1979**, *366*, 23.
 26. Dridi, Z.; Bouhafs, B.; Ruterana, P.; Aourag, H. *J. Phys.: Condens. Matter* **2002**, *14*, 10237.
 27. Pauling, L. *The Nature of the Chemical Bond*; Cornell University Press: Ithaca, New York, 1960.
 28. Chen, K. Y.; Zhao, L. R. *J. Phys. Chem. Solids* **2007**, *68*, 1805.
-